Sawtooth-like oscillations and steady states caused by the m/n=2/1 double tearing mode

W. Zhang[1], Z. W. Ma[1*], H. W. Zhang[1], and X. Wang[1]

[1]Institute for Fusion Theory and Simulation, Department of Physics, Zhejiang University, Hangzhou 310027, China

Abstract: The sawtooth-like oscillations resulting from the nonlinear evolution of the m/n=2/1 double tearing mode (DTM) are numerically investigated through the three-dimensional, toroidal, nonlinear resistive-MHD code (CLT). We find that the nonlinear evolution of the m/n=2/1 DTM can lead to sawtooth-like oscillations, which are similar to those driven by the kink mode. The perpendicular thermal conductivity and the external heating rate can significantly alter the behaviors of the DTM driven sawtooth-like oscillations. With the high perpendicular thermal conductivity, the system quickly evolves into the steady state with m/n=2/1 magnetic islands and helical flow. However, with the low perpendicular thermal conductivity, the system tends to exhibit sawtooth-like oscillations. With a sufficiently high or low heating rate, the system exhibits sawtooth-like oscillations, while with an intermediate heating rate, the system quickly evolves into a steady state. The pressure evolution of the sawtooth-like oscillations agrees well with that observed in EAST. At the steady state, there exist the non-axisymmetric magnetic field and strong radial flow, and both are with helicity of m/n=2/1. Like the steady state with m/n=1/1 radial flow, which is beneficial for preventing the Helium ash accumulation in the core region, the steady state with m/n=2/1 radial flow might also be a good candidate for the advanced steady-state operations in future fusion reactors. It is also found that the behaviors of the sawtooth-like oscillations are almost independent of Tokamak geometry, which implies that the steady state with saturated m/n=2/1 magnetic islands might exist in different Tokamaks.

[a)] Corresponding Author: zwma@zju.edu.cn

I. Introduction

Scenarios with internal transport barriers (ITB) associated with reversed magnetic shear are designed as one of the advanced steady-state operations in future fusion reactors [1, 2]. The reversed magnetic shear can suppress trapped electron modes[3] and ballooning modes[4], which significantly improves energy confinement[3, 5-7]. However, severe MHD instabilities, often observed in Tokamaks with the reversed magnetic shear, can significantly degrade the energy confinement. These MHD instabilities sometimes lead to periodical oscillations of the plasma pressure in the core region[8-13], which are similar to the sawtooth oscillations (or sawteeth). As a result, these periodic oscillations are named off-axis sawteeth for annular pressure crashes and on-axis sawteeth for core plasma pressure crashes [8, 13, 14], or continuous MHD activity[10].

The MHD instabilities studied in the references [8-13] are related to the double tearing mode (DTM) with $m \geq 2$, which is a typical MHD instability for the reversed shear system. To avoid confusion with the m/n=1 kink-driven sawtooth, we name the oscillations driven by $m \geq 2$ DTM as sawtooth-like behaviors or sawtooth-like oscillations in the present paper. It should be noted that, although the linear and nonlinear evolutions[15-23], as well as the nonlinearly explosive growth of DTM[24-32] and DTM suppression[33-42], have been intensively investigated, the periodic oscillations associated with the DTMs (i.e., sawtooth-like oscillations) are rarely numerically investigated.

In the present paper, we will focus on the characteristics of the sawtooth-like oscillations, including the period and the amplitude of the oscillations, the typical pressure profiles, and flow patterns during the oscillations. We find that the behaviors of the sawtooth-like oscillations can be altered with different perpendicular thermal conductivities or heating rates. With proper heating rate or high perpendicular thermal conductivity, the system quickly reaches a steady state with the non-axisymmetric magnetic field and strong radial flows, which is similar to the steady state observed in

the sawtooth oscillations driven by the kink instability.[43] However, the dominant mode is the m/n=2/1 DTM in the reversed magnetic shear configuration, while it is the m/n=1/1 kink mode in the monotonous q profile configuration. Like the m/n=1/1 steady state, the quasi-stationary state associated with m/n=2/1 DTM is also sawtooth free and can avoid severe pressure crashes. Meanwhile, the radial flow can help prevent Helium ash accumulation in the core region for future fusion reactors. Such kind of a steady state might be important for advanced operations in future fusion reactors.

II. Numerical model

The resistive-MHD equations utilized in CLT[44] are given as follows:

$$\frac{\partial \rho}{\partial t} = -\nabla \cdot (\rho \mathbf{v}) + \nabla \cdot [D \nabla (\rho - \rho_0)], \tag{1}$$

$$\frac{\partial p}{\partial t} = -\mathbf{v} \cdot \nabla p - \Gamma p \nabla \cdot \mathbf{v} + \nabla \cdot [\kappa_\perp \nabla p + \kappa_\parallel \nabla_\parallel p] - \nabla \cdot [H_0 \nabla p_0], \tag{2}$$

$$\frac{\partial \mathbf{v}}{\partial t} = -\mathbf{v} \cdot \nabla \mathbf{v} + (\mathbf{J} \times \mathbf{B} - \nabla p) / \rho + \nabla \cdot [\nu \nabla (\mathbf{v})], \tag{3}$$

$$\frac{\partial \mathbf{B}}{\partial t} = -\nabla \times \mathbf{E}, \tag{4}$$

$$\mathbf{E} = -\mathbf{v} \times \mathbf{B} + \eta (\mathbf{J} - \mathbf{J}_0), \tag{5}$$

$$\mathbf{J} = \frac{1}{\mu_0} \nabla \times \mathbf{B}, \tag{6}$$

where ρ, p, $\mathbf{v}$, $\mathbf{J}$, $\mathbf{B}$, and $\mathbf{E}$ are the plasma density, the plasma pressure, the fluid velocity, the current density, the magnetic field, and the electric field, respectively. The subscript "0" denotes the initial quantities. $\Gamma (= 5/3)$ is the ratio of specific heat of the plasma. In CLT, the electric field is used as an intermediate variable for the purpose of keeping $\nabla \cdot \mathbf{B} = 0$. All the variables are normalized as follows: $\mathbf{x} / a \to \mathbf{x}$, $t / t_A \to t$, $\rho / \rho_{00} \to \rho$, $p / (B_{00}^2 / \mu_0) \to p$, $\mathbf{v} / v_A \to \mathbf{v}$, $\mathbf{J} / (B_{00} / \mu_0 a) \to \mathbf{J}$, $\mathbf{B} / B_{00} \to \mathbf{B}$, and

$\mathbf{E}/(v_A B_{00}) \to \mathbf{E}$, respectively. B_{00} and ρ_{00} are the initial magnetic field and the plasma density at the magnetic axis, respectively. a is the minor radius, $v_A = B_{00}/\sqrt{\mu_0 \rho_{00}}$ is the Alfvén speed, and $t_A = a/v_A$ is the Alfvén time. η, D, $\kappa_\perp$, $\kappa_\parallel$, H_0 and υ are the resistivity, the diffusion coefficient, the perpendicular and parallel thermal conductivity, the heating rate, and the viscosity, respectively, which are normalized as follows: $\eta/(\mu_0 a^2/t_A) \to \eta$, $D/(a^2/t_A) \to D$, $\kappa_\perp/(a^2/t_A) \to \kappa_\perp$, $\kappa_\parallel/(a^2/t_A) \to \kappa_\parallel$, $H_0/(a^2/t_A) \to H_0$, and $\nu/(a^2/t_A) \to \nu$.

Since the present paper investigates the sawtooth-like oscillations, external heating sources are needed so that the oscillations can continue. For simplicity, we assume that all external heating sources are included in the last term in Eq. (2). Such a form of an external source always heats the plasma towards a peak distribution of the plasma, and the heating rate is proportional to H_0. Meanwhile, we add a source term in Ohm's law (Eq. (5)), and this term acts as the flux pump so that the magnetic surface could restore the initial status after crashes.

III. Simulation results

A. The sawtooth-like oscillations

The most recent experimental observations of sawtooth-like oscillations caused by the nonlinear evolution of the m/n=2/1 DTM are reported by the EAST team.[13, 45] In the present paper, we utilize similar parameters from EAST, i.e., the major radius $R_0 = 1.85m$, the minor radius $a = 0.45m$, the elongation E=1.9, the triangularity $\sigma = 0.5$, the toroidal field $\mathbf{B_T} \sim 2T$, and the plasma current $I_p \sim 0.7MA$. We also choose a typical q profile with the reversed magnetic shear for the m/n=2/1 DTM. The initial q profile and pressure profile are shown in Figure 1. The distance between the two q=2 resonant surfaces are $\Delta r = 0.35a$. The initial equilibrium is derived from the QSOLVER code.[46] Other normalized parameters used in this subsection are chosen

to be $\eta=3\times10^{-6}$, $D=1\times10^{-4}$, $\kappa_{\perp}=3\times10^{-6}$, $\kappa_{\parallel}=5\times10^{-2}$, $H_0=3\times10^{-6}$, and $\nu=3\times10^{-5}$. The grids used in the simulations are $256\times32\times256$ (R,φ,Z). The convergence studies have also been carried out with different time steps and spatial resolutions.

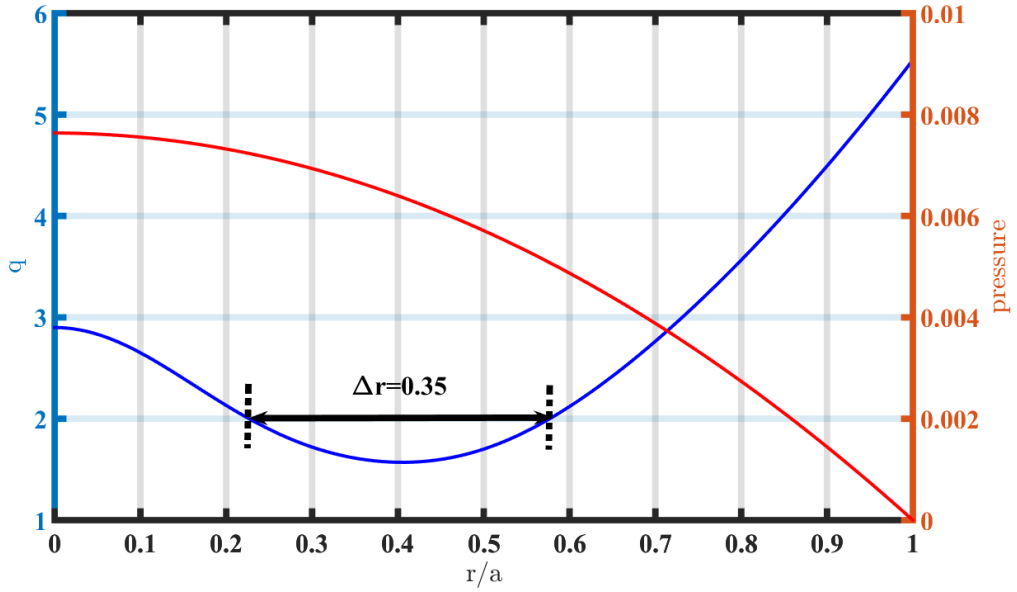

Figure 1 Initial q profile and pressure profile.

The time evolutions of the kinetic energy for different toroidal modes are shown in Figure 2. It indicates that the kinetic energies for all toroidal modes experience periodical oscillations. The oscillation period of the kinetic energy is about $4500\,t_A$. We further decompose the n=1 component with different poloidal mode numbers m. The evolution of $E_{\phi mn}$ is shown in Figure 3. The dominant mode is the m/n=2/1 mode, which confirms that the m/n=2/1 DTM drives the oscillations. Not only the kinetic energy, other characteristics such as the on-axis plasma pressure also periodically oscillate with the same period $T\sim4500t_A$, as shown in Figure 4. The simulation results are similar to the oscillations observed in EAST[13], JET[12], ASDEX-U[10], Rijnhuizen Tokamak[9], and TFTR[8]. It is evident that although the system has no q=1

resonant surface, it still could experience periodical oscillations. The behavior is somewhat similar to sawteeth driven by the m/n=1/1 resistive-kink mode, but the dominant mode is the m/n=2/1 DTM.

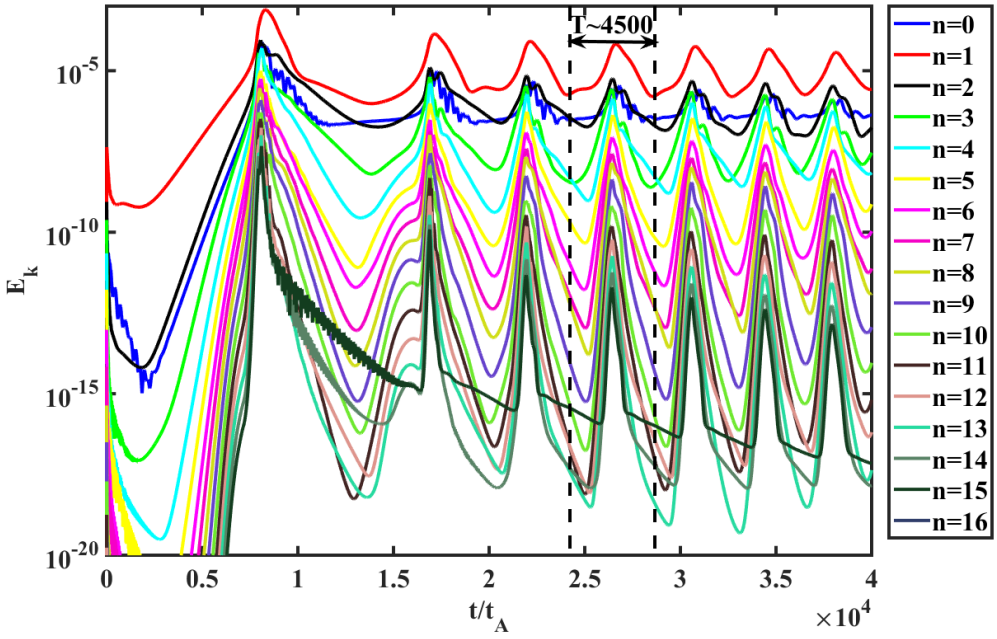

Figure 2 The time evolutions of the kinetic energy for different toroidal modes. It is evident that all modes experience periodic oscillations, and their periods are the same, $T \sim 4500 t_A$.

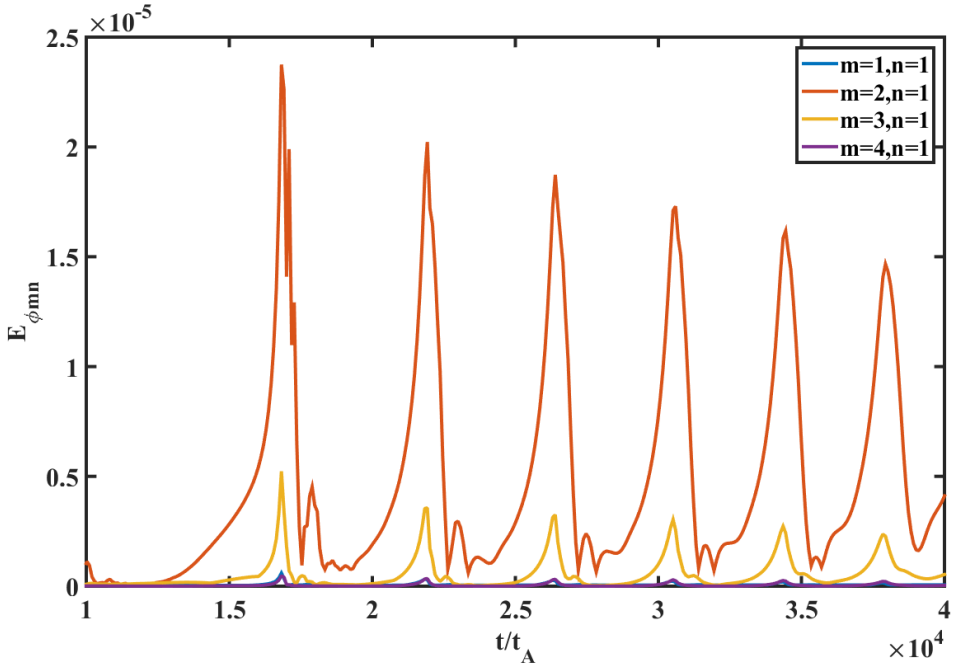

Figure 3 The evolution of the toroidal electric field $E_{\phi mn}$. Since the modes with different mode numbers are located at different radius, we choose the maximum $E_{\phi mn}$ at each time step to indicate the amplitudes of the modes. The m/n=2/1 mode is the dominant one throughout the simulation.

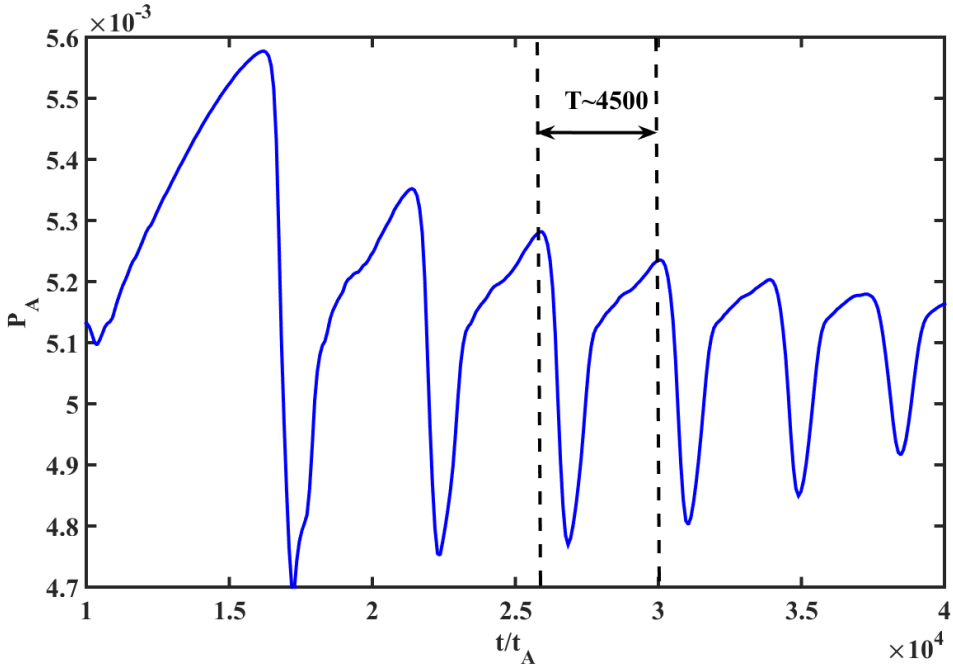

Figure 4 The evolution of the on-axis plasma pressure. It is evident that the on-axis

plasma pressure also experiences periodical oscillations with the period $T \sim 4500 t_A$.

Snapshots of the Poincare plots of magnetic field lines during one sawtooth cycle are shown in Figure 5, which confirms that the m/n=2/1 DTM drives the sawtooth-like oscillations. At $t = 25054 t_A$ (Figure 5a), large m/n=2/1 magnetic islands at the two q=2 resonant surfaces form, which is the precursor of the pressure crash. It should be noted that the plasma in the inner islands is hot while it is cold in the outer islands. Just before the pressure crash (Figure 5b and c), the inner islands are gradually expelled outward due to the inward expansion of the outer islands. As a result, the hot plasma core finally squeezed out from the core region (Figure 5d). This is one of the basic features of the on-axis pressure crash, which is similar to the experimental observations[8, 13]. After the severe pressure crashes, the external heating and magnetic pump in Eq. (2) and Eq. (5) become dominant, the system gradually recovers (Figure 5d), and a new cycle begins (Figure 5e and f).

We have plotted the contour plots of the plasma pressure with the flow pattern at the same moments in Figure 5. During the DTM precursor (Figure 6a), the plasma pressure profile becomes flattened inside the islands, and the plasma flows generated by the reconnection process are weak. Just before the pressure crash (Figure 6b and c), an elongated hot plasma region forms due to the inward expansion of the outer islands, as shown in Figures 5b and 5c. Meanwhile, strong radial flow is generated along this hot plasma region.[31] This radial flow quickly transfers the hot plasma from the core region to the outer region and leads to the on-axis pressure crash. Thereafter, the radial flow is dissipated, and the on-axis plasma pressure starts to recover due to external heating.

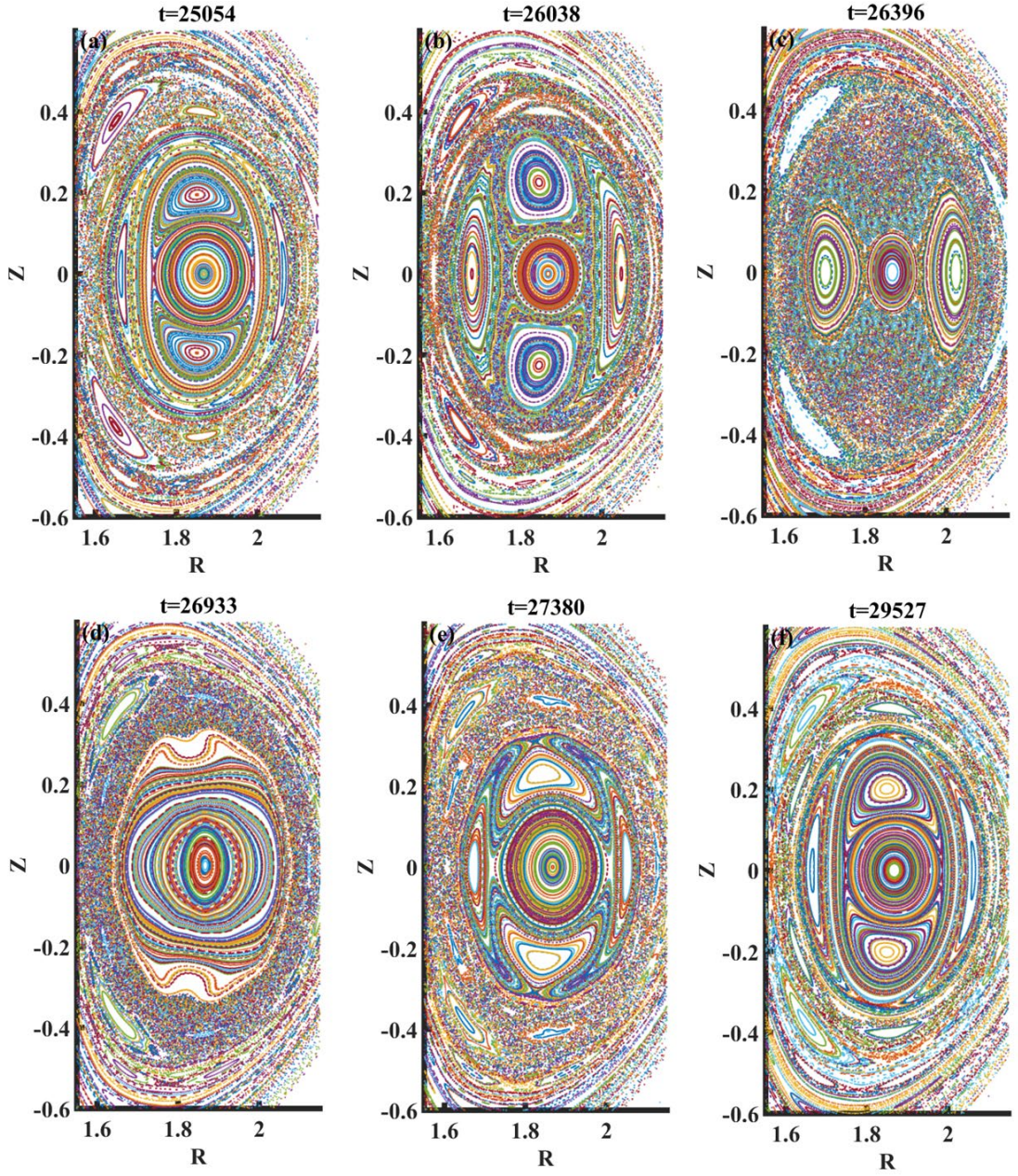

Figure 5 Snapshots of the Poincare plots of the magnetic field lines during one sawtooth cycle.

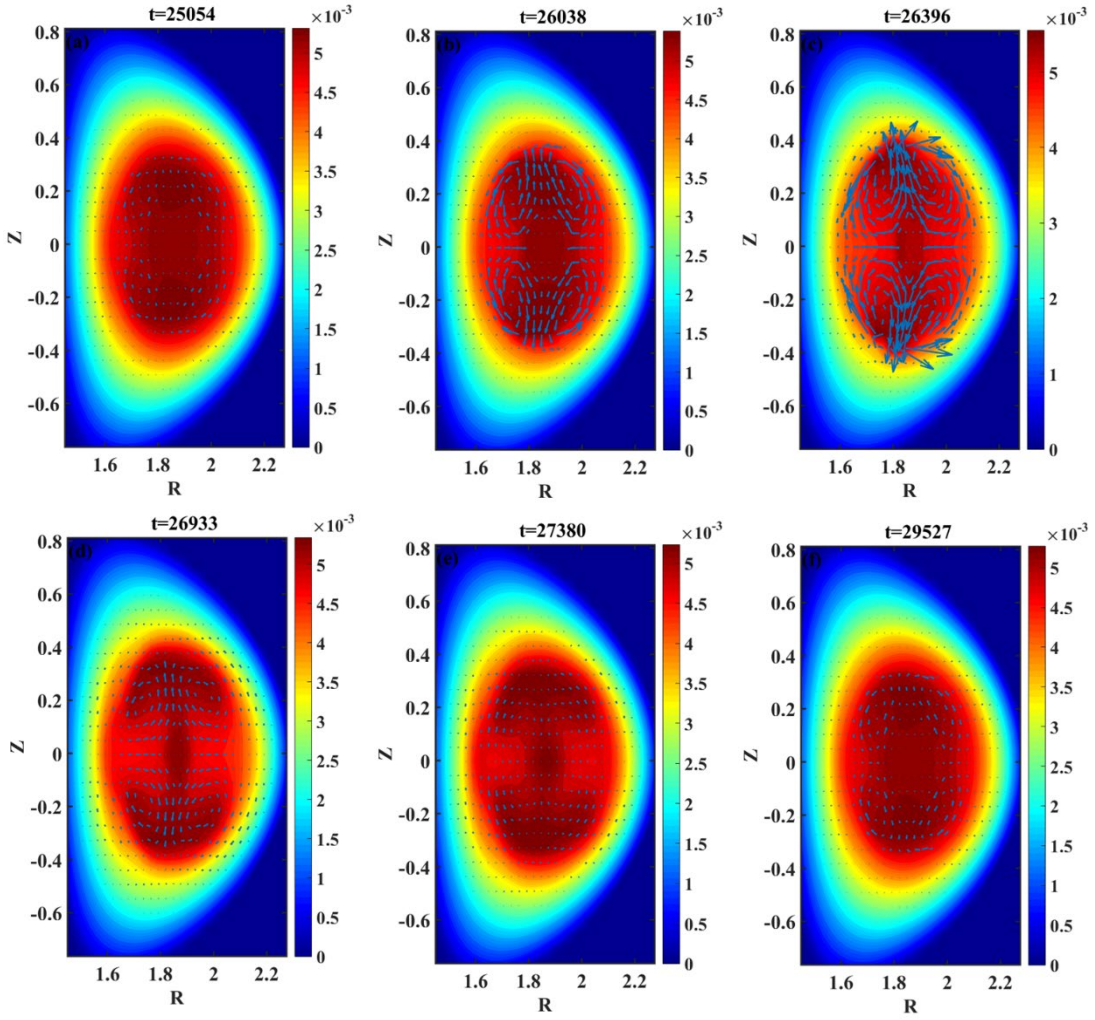

Figure 6 The contour plots of the plasma pressure with the flow patterns at the same moments in Figure 5. The vector length in each figure has been normalized by the maximum value in Figure 6c.

B. The sawtooth-like oscillations and the steady states associated with the m/n=2/1 DTM

As shown in our previous studies, the plasma parameters (such as the viscosity) can significantly influence the kink-driven sawteeth's behaviors. [43] The system can even achieve a steady state with a saturated m/n=1/1 magnetic island with a low viscosity. At the steady state, the sawtooth-free system can avoid severe pressure crashes. As a result, it might be important for Tokamak operations.[47] The steady state with the m/n=1/1 magnetic island has been widely investigated, but the steady state driven by the DTM has rarely been discussed in the literature.

In this subsection, we keep the heating rate to be the same with the perpendicular diffusion rate (i.e., $\kappa_\perp = H_0$), and scan from $\kappa_\perp = H_0 = 1\times10^{-6}$ to $\kappa_\perp = H_0 = 3\times10^{-5}$. As shown in Figure 7, the behaviors of the sawtooth-like oscillations are significantly different. The amplitude of the pressure crash increase with increasing $\kappa_\perp = H_0$. For $\kappa_\perp = H_0 = 1\times10^{-6}$, the amplitude of the pressure crash is only about 3%, while for $\kappa_\perp = H_0 = 3\times10^{-5}$, it is more than 20%. This is because, with the low heating $\kappa_\perp = H_0 = 1\times10^{-6}$, the system is weakly heated before the next crash. As a result, the amplitude of the pressure crash is small.

It is interesting that the on-axis pressure quickly reaches a steady state with $\kappa_\perp = H_0 = 3\times10^{-5}$ as shown in Figure 7. This could also be seen from the kinetic energy evolution with $\kappa_\perp = H_0 = 3\times10^{-5}$ (Figure 8). The system quickly reaches a steady state after several cycles, and all the modes keep unchanged since then. As one can see, these behaviors are similar to the steady state with the m/n=1/1 magnetic island. However, as shown in Figure 9 and Figure 10, the system at the steady state has saturated m/n=2/1 magnetic islands and plasma flow, which is different from the steady state with the m/n=1/1 magnetic island.

As discussed by many previous studies, [48]the sawtooth-free steady state can not only avoid the pressure crash but also prevent impurity accumulations in the core region since the radial flow carries both plasma and impurity from the core to the outer region. It is implied that the steady state with the m/n=2/1 DTM might also be a proper candidate for the high confinement operation.

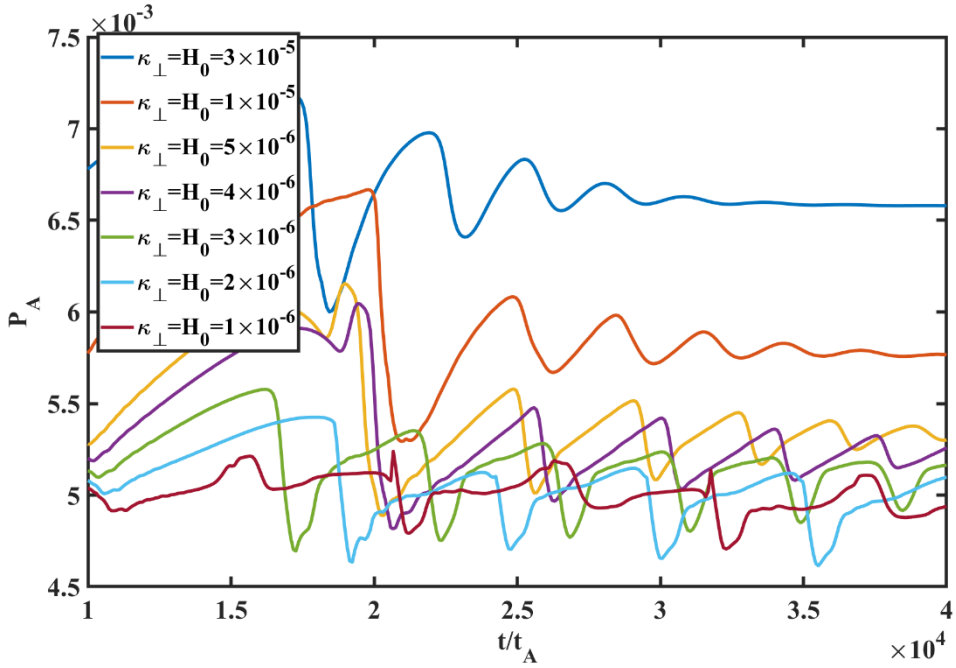

Figure 7 The evolutions of the on-axis plasma pressure with different $\kappa_\perp = H_0$.

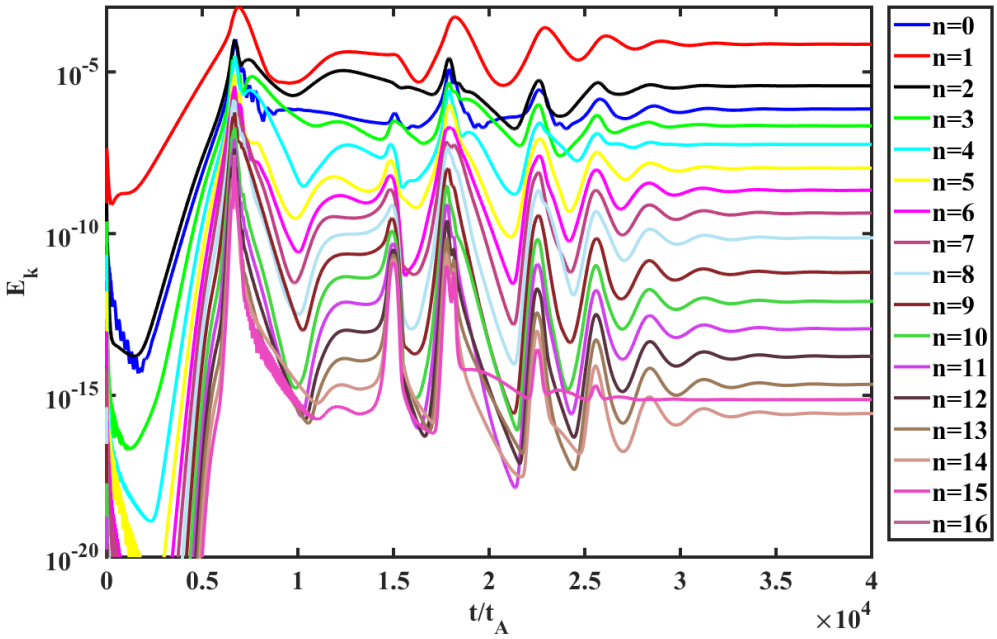

Figure 8 The kinetic energy evolution of the different toroidal mode numbers with $\kappa_\perp = H_0 = 3\times10^{-5}$. The system reaches a steady state after $t \sim 30000 t_A$.

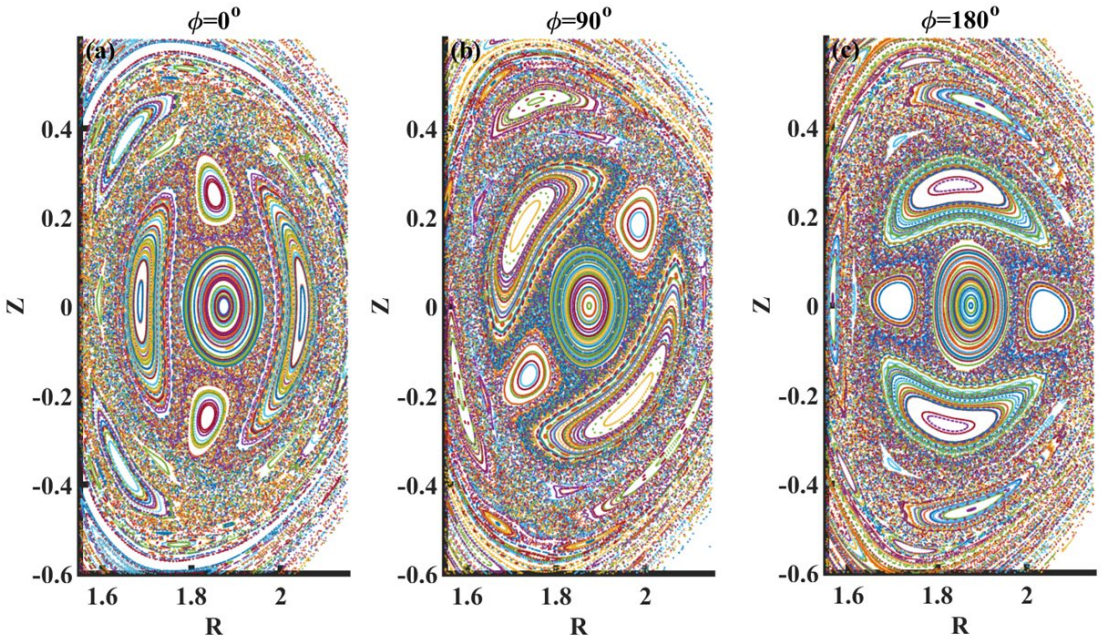

Figure 9 The Poincare plots of magnetic field lines at the steady state at $\phi = 0^o$, $\phi = 90^o$, and $\phi = 180^o$ in the EAST geometry.

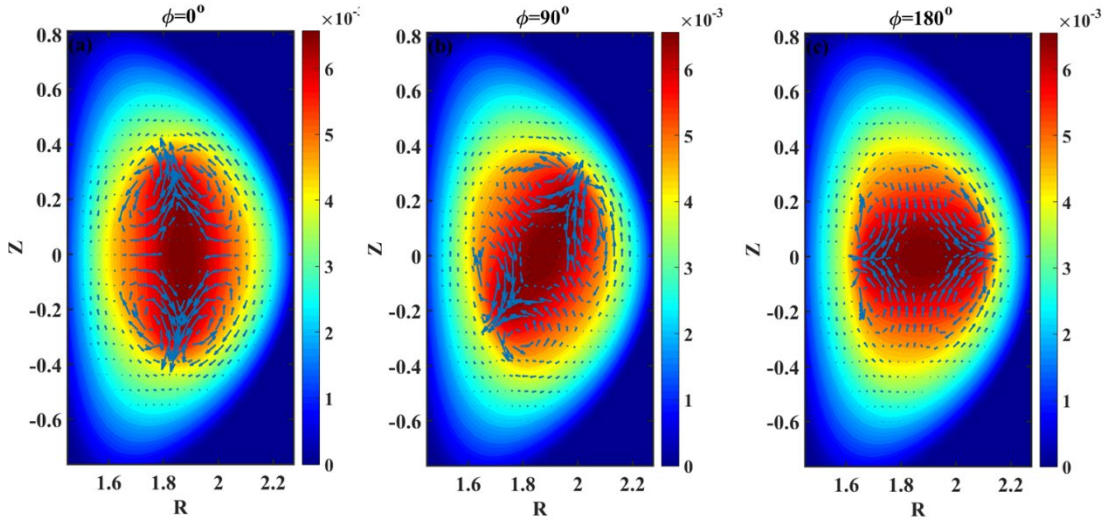

Figure 10 The flow patterns and pressure profiles at the steady state at $\phi = 0^o$, $\phi = 90^o$, and $\phi = 180^o$ in the EAST geometry.

C. The influence of the perpendicular thermal conductivity and the heating rate on the sawtooth-like oscillations.

As shown in Subsection III. B, the behaviors of the sawtooth-like oscillations are

sensitive to the perpendicular thermal conductivity and the heating rate. However, it is still not clear which parameter is the dominant one because we assume $\kappa_\perp = H_0$ for simplification. In this subsection, we will investigate the influence of the two parameters separately.

To study the influence of the perpendicular thermal conductivity, we scan from $\kappa_\perp = 1\times10^{-6}$ to $\kappa_\perp = 3\times10^{-5}$, and keep $H_0 = 3\times10^{-6}$. As shown in Figure 11, the perpendicular thermal conductivity could largely alter the behaviors of the sawtooth-like oscillations. For example, with $\kappa_\perp = 3\times10^{-5}$, the total kinetic energy quickly saturates, and the system reaches a steady state. While, with $\kappa_\perp = 1\times10^{-6}$, the system exhibits good periodicity. The evolutions of the on-axis plasma pressure for the fixed heating rate ($H_0 = 3\times10^{-6}$) with different perpendicular thermal conductivities are shown in Figure 12 that clearly indicates that the system is more easily to evolve into the steady state with a high perpendicular thermal conductivity.

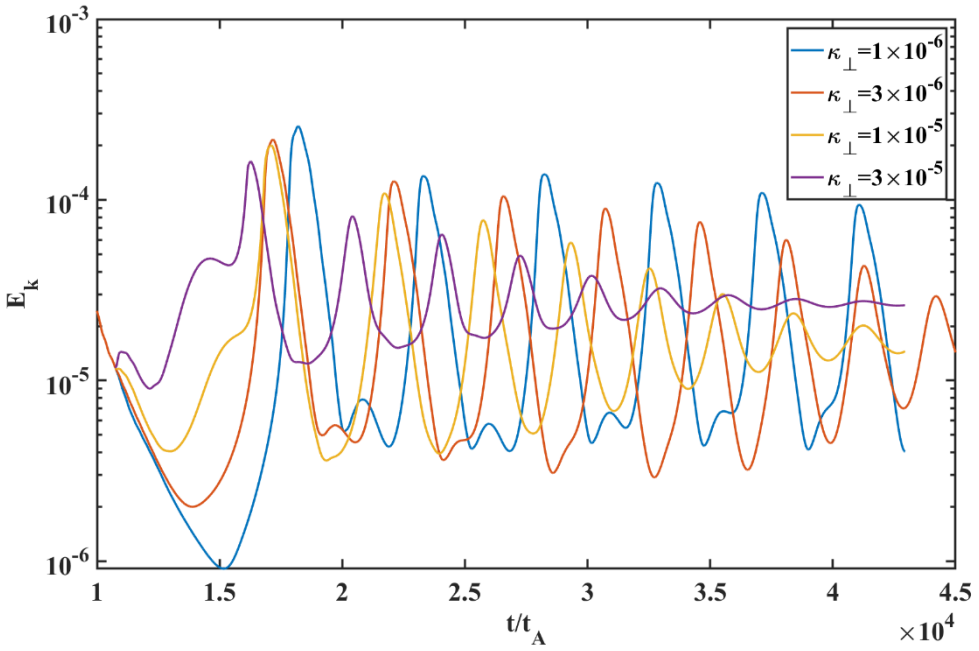

Figure 11 The evolutions of the total kinetic energy for the fixed heating rate ($H_0 = 3\times10^{-6}$) with different perpendicular thermal conductivities.

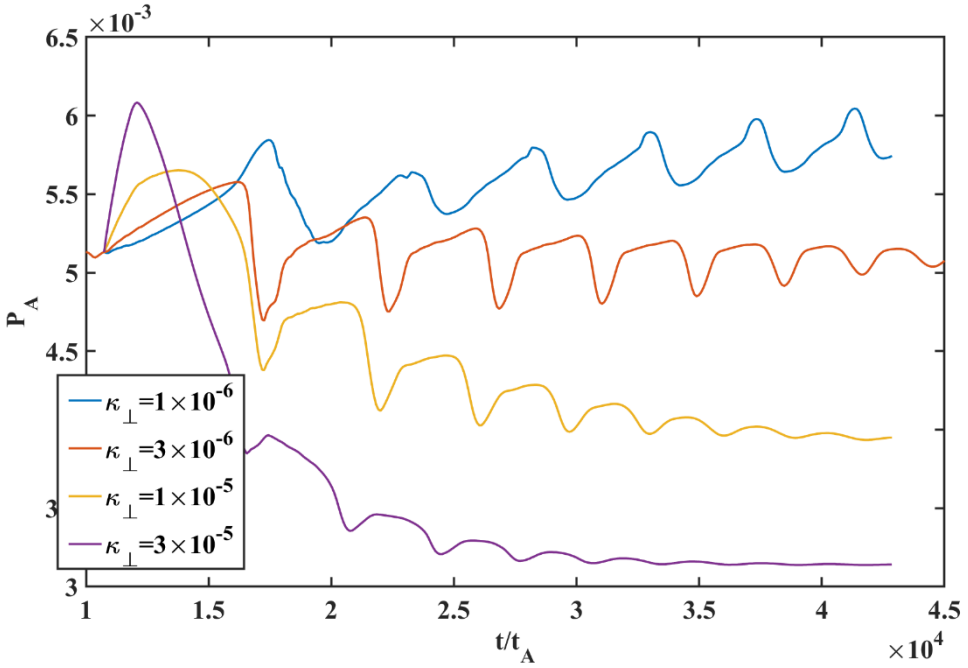

Figure 12 The evolutions of the on-axis plasma pressure for the fixed heating rate ($H_0 = 3\times10^{-6}$) with different perpendicular thermal conductivities.

Similarly, to investigate the influence of the heating rate, we scan from $H_0 = 1\times10^{-6}$ to $H_0 = 2\times10^{-5}$ with the fixed conductivity $\kappa_\perp = 3\times10^{-6}$. The evolutions of the total kinetic energy for the fixed perpendicular thermal conductivity ($\kappa_\perp = 3\times10^{-6}$) with different heating rates are shown in Figure 13. We find that, with a moderate heating rate (i.e. $H_0 = 1\times10^{-5}$), the system can evolve to the steady state. However, with a relatively high or low heating rate, the system exhibits a sawtooth-like oscillation. Such tendency can also be seen from the evolutions of the on-axis plasma pressure as shown in Figure 14.

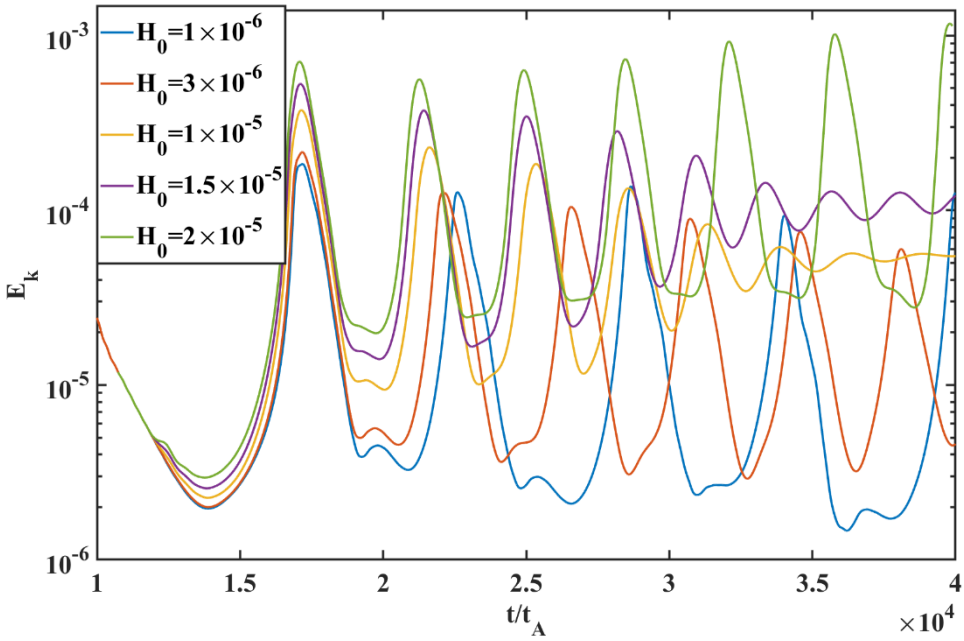

Figure 13 The evolutions of the total kinetic energy for the fixed perpendicular thermal conductivity ($\kappa_{\perp} = 3\times10^{-6}$) with different heating rates.

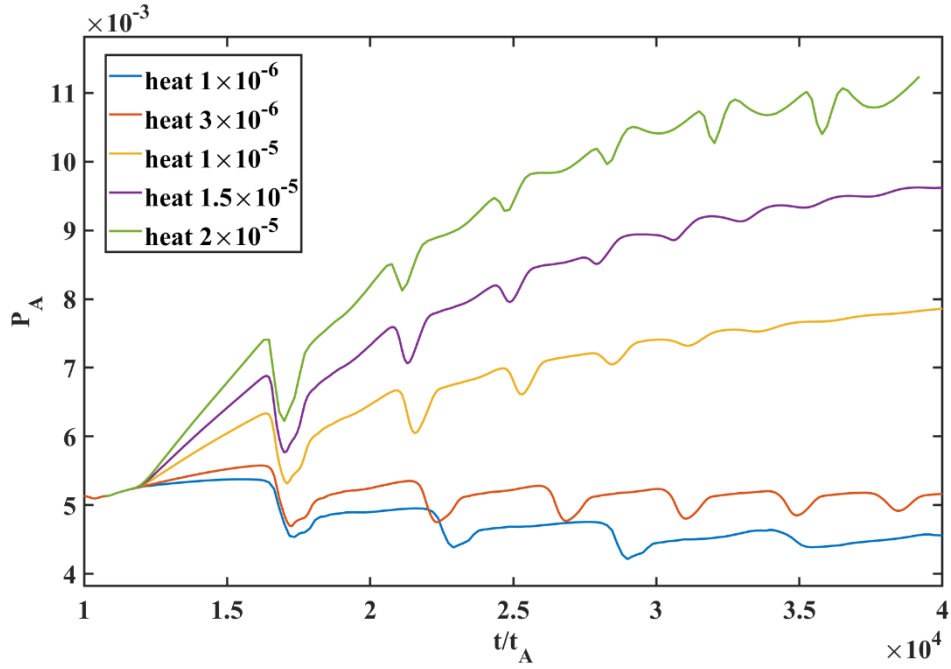

Figure 14 The evolutions of the on-axis plasma pressure for the fixed perpendicular thermal conductivity ($\kappa_{\perp} = 3\times10^{-6}$) with different heating rates

D. The sawtooth-like oscillations in the ITER geometry

In this subsection, we utilize similar parameters from ITER to investigate the sawtooth-like behaviors in ITER. The major radius $R_0 = 6.20m$, the minor radius $a = 2.0m$, the elongation E=1.7, the triangularity $\sigma = 0.3$. Since we only focus on the internal instabilities, the simulation boundary is chosen to be the last closed surface in the present paper. The initial q and pressure profiles vs. the minor radius are the same with Figure 1, and other normalized parameters are also kept the same as in Section III. B. With the ITER geometry, the on-axis plasma pressure evolutions with different $\kappa_\perp = H_0$ are qualitatively the same as EAST. As shown in Figure 15, the system exhibits the sawtooth-like oscillation with $\kappa_\perp = H_0 = 3\times10^{-6}$, while, it quickly reaches the steady state with $\kappa_\perp = H_0 = 3\times10^{-5}$. Similarly, the strong radial flow and the large m/n=2/1 magnetic islands exist at the steady state (Figure 16 and 17).

We have also carried out simulations to investigate the sawtooth-like oscillations with different Tokamak geometries (the ASDEX-U and TFTR). Since the results are qualitatively the same, we do not present these similar results in the present paper. These studies indicate that different Tokamak geometries only weakly affect the behaviors of the sawtooth-like oscillations.

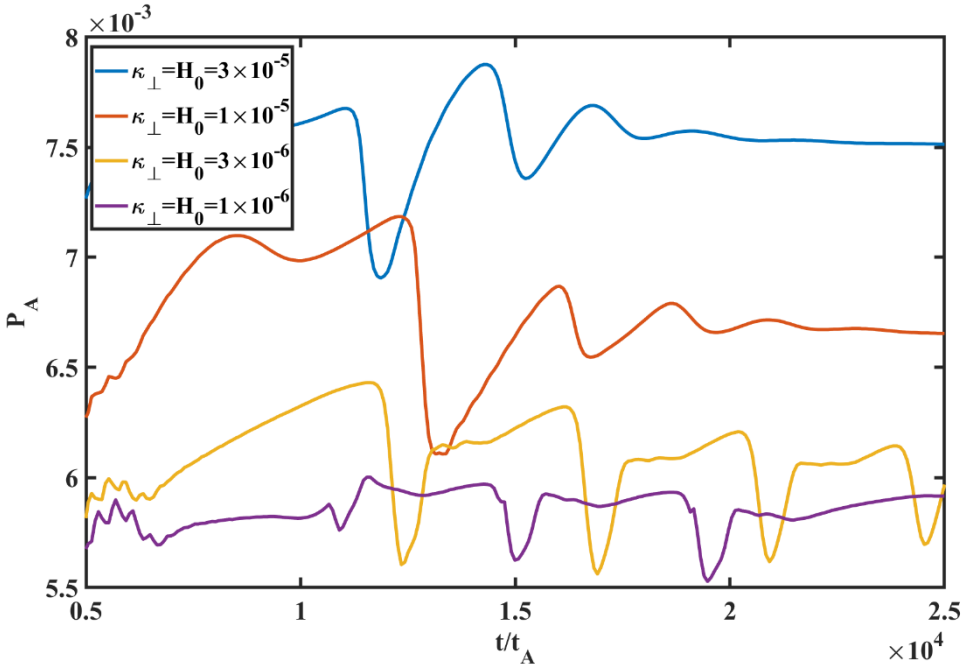

Figure 15 The evolutions of the on-axis plasma pressure with the different $\kappa_{\perp} = H_0$ in the ITER geometry simulations.

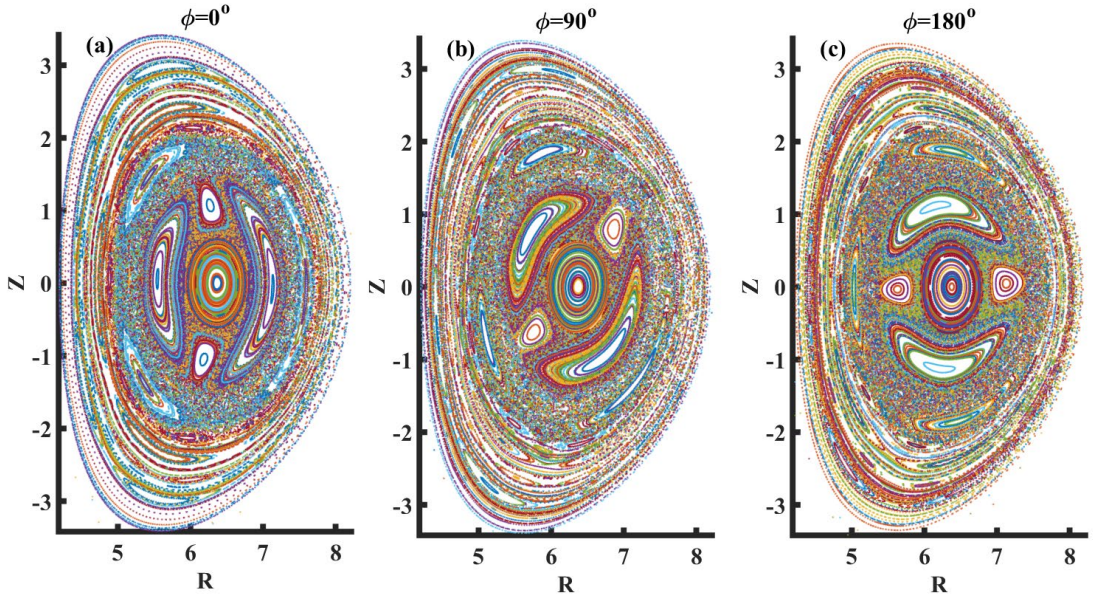

Figure 16 The Poincare plots of magnetic field lines at the steady state at $\phi = 0^o$, $\phi = 90^o$, and $\phi = 180^o$ in the ITER geometry.

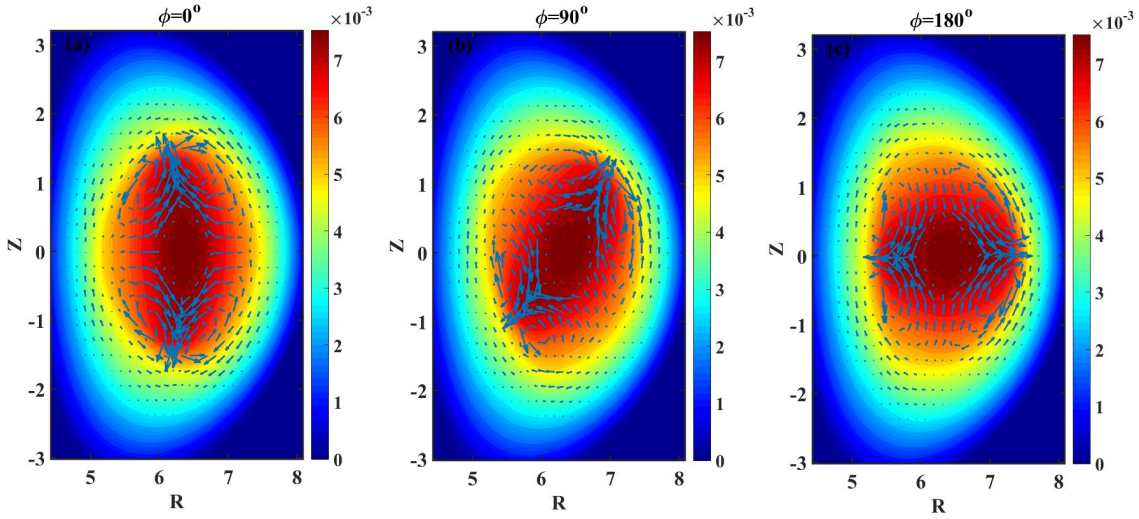

Figure 17 The flow patterns and pressure profiles at the steady state at $\phi = 0^o$, $\phi = 90^o$, and $\phi = 180^o$ in the ITER geometry.

IV. Discussions and conclusions

The sawtooth-like oscillations driven by the m/n=2/1 DTM are numerically investigated through the three-dimensional, toroidal, nonlinear resistive-MHD code CLT. Similar to the kink-driven sawtooth oscillations, both the kinetic energy and the on-axis plasma pressure oscillate with the same period. The dominant mode is the m/n=2/1 DTM throughout the oscillation periods. The evolutions of the on-axis pressure and the pressure profiles are consistent with the observations in EAST.[13, 45]

We have systematically investigated the influence of the heating rate H_0 and the perpendicular thermal conductivity on the behaviors of the sawtooth-like oscillations. We find that, with a higher perpendicular thermal conductivity, the system is more easily to evolve into the steady state; however, with a low perpendicular thermal conductivity, the system tends to exhibit sawtooth-like oscillations. We also find that the behaviors of the sawtooth-like oscillations can be altered by imposing different heating rates. With a relatively high or low heating rate, the system exhibits sawtooth-like oscillations, while, the system quickly evolves into the steady state with an intermediate heating rate.

At the steady state, the system has a non-axisymmetric magnetic field and a strong

radial flow, which is similar to the steady state observed in the kink-driven sawtooth oscillations.[43] The helicity of the saturated magnetic islands and the plasma flow is m/n=2/1 for the DTM dominant steady state, while it is m/n=1/1 for the kink mode dominant steady state. As we know, the radial flow can help to expel the Helium ash, and thus prevent Helium ash from accumulating in the hot core. Even more, the sawtooth-free steady state will not experience severe pressure crashes naturally. Like the steady state with the m/n=1/1 magnetic island, the steady state with the m/n=2/1 DTM is also beneficial to preventing Helium ash accumulation in the core region and avoiding the severe pressure crash. It implies that such kind of the scenario might be important for future fusion reactors. We have also carried out systematical simulations to investigate the sawtooth-like oscillations with different Tokamak geometries. We find that the behaviors of the sawtooth-like oscillations and the steady state are qualitatively the same in different Tokamak geometries. Therefore, we believe that the steady state, with the dominant mode m/n=2/1 DTM, could widely exist in present Tokamaks.

Acknowledgment

This work is supported by the National MCF Energy R&D Program No. 2019YFE03090500, the National Natural Science Foundation of China under Grant No. 12005185, 11775188 and 11835010, Fundamental Research Fund for Chinese Central Universities No. 2021FZZX003-03-02.

Reference:

[1] Y.X. Wan, J.G. Li, Y. Liu, X.L. Wang, C. Vincent, C.G. Chen, X.R. Duan, P. Fu, X. Gao, K.M. Feng, S.I. Liu, Y.T. Song, P.D. Weng, B.N. Wan, F.R. Wan, H.Y. Wang, S.T. Wu, M.Y. Ye, Q.W. Yang, G.Y. Zheng, G. Zhuang, Q. Li, C. team, Overview of the present progress and activities on the CFETR, Nuclear Fusion, 57 (2017) 102009.

[2] A.C.C. Sips, f.t.S.S. Operation, t.T.P.t.g. Activity, Advanced scenarios for ITER Plasma Physics and Controlled Fusion, 47 (2005) A19-A40.

[3] C. Kessel, J. Manickam, G. Rewoldt, W.M. Tang, Improved plasma performance in tokamaks with negative magnetic shear, Physical Review Letters, 72 (1994) 1212-1215.

[4] A. Sykes, J.A. Wesson, S.J. Cox, High-$\ensuremath{\beta}$ Tokamaks, Physical Review Letters, 39 (1977) 757-760.

[5] F.M. Levinton, M.C. Zarnstorff, S.H. Batha, M. Bell, R.E. Bell, R.V. Budny, C. Bush, Z. Chang, E. Fredrickson, A. Janos, J. Manickam, A. Ramsey, S.A. Sabbagh, G.L. Schmidt, E.J. Synakowski, G. Taylor, Improved Confinement with Reversed Magnetic Shear in TFTR, Physical Review Letters, 75 (1995) 4417-4420.
[6] E.J. Strait, L.L. Lao, M.E. Mauel, B.W. Rice, T.S. Taylor, K.H. Burrell, M.S. Chu, E.A. Lazarus, T.H. Osborne, S.J. Thompson, A.D. Turnbull, Enhanced Confinement and Stability in DIII-D Discharges with Reversed Magnetic Shear, Physical Review Letters, 75 (1995) 4421-4424.
[7] H. Kishimoto, S. Ishida, M. Kikuchi, H. Ninomiya, Advanced tokamak research on JT-60, Nuclear Fusion, 45 (2005) 986.
[8] Z. Chang, W. Park, E.D. Fredrickson, S.H. Batha, M.G. Bell, R. Bell, R.V. Budny, C.E. Bush, A. Janos, F.M. Levinton, K.M. McGuire, H. Park, S.A. Sabbagh, G.L. Schmidt, S.D. Scott, E.J. Synakowski, H. Takahashi, G. Taylor, M.C. Zarnstorff, Off-Axis Sawteeth and Double-Tearing Reconnection in Reversed Magnetic Shear Plasmas in TFTR, Physical Review Letters, 77 (1996) 3553-3556.
[9] M.R. de Baar, G.M.D. Hogeweij, N.J. Lopes Cardozo, A.A.M. Oomens, F.C. Schüller, Electron Thermal Transport Barrier and Magnetohydrodynamic Activity Observed in Tokamak Plasmas with Negative Central Shear, Physical Review Letters, 78 (1997) 4573-4576.
[10] S. Günter, S. Schade, M. Maraschek, S.D. Pinches, E. Strumberger, R. Wolf, Q. Yu, A.U. Team, MHD phenomena in reversed shear discharges on ASDEX Upgrade, Nuclear Fusion, 40 (2000) 1541.
[11] C.D. Challis, Y.F. Baranov, G.D. Conway, C. Gormezano, C.W. Gowers, N.C. Hawkes, T.C. Hender, E. Joffrin, J. Mailloux, D. Mazon, S. Podda, R. Prentice, F.G. Rimini, S.E. Sharapov, A.C.C. Sips, B.C. Stratton, D. Testa, K.D. Zastrow, Effect ofq-profile modification by LHCD on internal transport barriers in JET*, Plasma Physics and Controlled Fusion, 43 (2001) 861-879.
[12] G.M.D. Hogeweij, Y. Baranov, G.D. Conway, S.R. Cortes, M.R.D. Baar, N. Hawkes, F. Imbeaux, X. Litaudon, J. Mailloux, F.G. Rimini, S.E. Sharapov, B.C. Stratton, K.D. Zastrow, c.t.t.E.-J.E.T. workprogramme, Electron heated internal transport barriers in JET*, Plasma Physics and Controlled Fusion, 44 (2002) 1155-1165.
[13] M. Xu, H.L. Zhao, Q. Zang, G.Q. Zhong, L.Q. Xu, H.Q. Liu, W. Chen, J. Huang, L.Q. Hu, G.S. Xu, X.Z. Gong, J.P. Qian, Y. Liu, T. Zhang, Y. Zhang, Y.W. Sun, X.D. Zhang, B.N. Wan, Characteristics of off-axis sawteeth with an internal transport barrier in EAST, Nuclear Fusion, 59 (2019) 084005.
[14] M. Xu, H.L. Zhao, J.Z. Zhang, L.Q. Xu, H.Q. Liu, G.Q. Li, G.Q. Zhong, Q. Zang, L.Q. Hu, X.Z. Gong, G.S. Xu, X.D. Zhang, B.N. Wan, E. team, Excitation of the beta-induced Alfvén-acoustic eigenmode during sawtooth-like oscillation in EAST, Nuclear Fusion, 60 (2020) 112005.
[15] P.L. Pritchett, Y.C. Lee, J.F. Drake, Linear analysis of the double-tearing mode, The Physics of Fluids, 23 (1980) 1368-1374.
[16] B. Carreras, H.R. Hicks, B.V. Waddell, Tearing-mode activity for hollow current profiles, Nuclear Fusion, 19 (1979) 583.
[17] E. Fredrickson, M. Bell, R.V. Budny, E. Synakowski, Nonlinear evolution of double tearing modes in tokamaks, Physics of Plasmas, 7 (2000) 4112-4120.
[18] Q. Yu, S. Günter, Numerical modelling of neoclassical double tearing modes, Nuclear Fusion, 39 (1999) 487.
[19] Y. Ishii, M. Azumi, G. Kurita, T. Tuda, Nonlinear evolution of double tearing modes, Physics of Plasmas, 7 (2000) 4477-4491.
[20] C.L. Zhang, Z.W. Ma, Nonlinear evolution of double tearing mode in Hall

magnetohydrodynamics, Physics of Plasmas, 16 (2009) 122113.
[21] M. Janvier, Y. Kishimoto, J. Li, Critical parameters for the nonlinear destabilization of double tearing modes in reversed shear plasmas, Nuclear Fusion, 51 (2011) 083016.
[22] Z.-X. Wang, L. Wei, F. Yu, Nonlinear evolution of neo-classical tearing modes in reversed magnetic shear tokamak plasmas, Nuclear Fusion, 55 (2015) 043005.
[23] W. Zhang, X. Lin, Z.W. Ma, X.Q. Lu, H.W. Zhang, The off-axis pressure crash associated with the nonlinear evolution of the m/n = 2/1 double tearing mode, Physics of Plasmas, 27 (2020) 122509.
[24] Y. Ishii, M. Azumi, Y. Kishimoto, Structure-Driven Nonlinear Instability of Double Tearing Modes and the Abrupt Growth after Long-Time-Scale Evolution, Physical Review Letters, 89 (2002) 205002.
[25] Z.X. Wang, X.G. Wang, J.Q. Dong, Y.A. Lei, Y.X. Long, Z.Z. Mou, W.X. Qu, Fast Resistive Reconnection Regime in the Nonlinear Evolution of Double Tearing Modes, Physical Review Letters, 99 (2007) 185004.
[26] M. Janvier, Y. Kishimoto, J.Q. Li, Structure-Driven Nonlinear Instability as the Origin of the Explosive Reconnection Dynamics in Resistive Double Tearing Modes, Physical Review Letters, 107 (2011) 195001.
[27] W. Zhang, Z.W. Ma, J. Zhu, H.W. Zhang, Core-crash sawtooth associated with m/n = 2/1 double tearing mode in Tokamak, Plasma Physics and Controlled Fusion, 61 (2019) 075002.
[28] J. Ma, W. Guo, Z. Yu, Q. Yu, Effect of plasmoids on nonlinear evolution of double tearing modes, Nuclear Fusion, 57 (2017) 126004.
[29] W. Guo, J. Ma, Q. Yu, Numerical study on nonlinear growth of m/n = 3/1 double tearing mode in high Lundquist number regime, Plasma Physics and Controlled Fusion, 61 (2019) 075011.
[30] A. Mao, Z. Wang, X. He, X. Wang, Nonlinear evolution and secondary island formation of the double tearing mode in a hybrid simulation, Plasma Science and Technology, 23 (2021) 035103.
[31] W. Zhang, Z.W. Ma, H.W. Zhang, Numerical Studies of Fast Pressure Crash Associated with Double Tearing Modes, Journal of Fusion Energy, 39 (2020) 367-381.
[32] Y.C. Feng, X.Q. Wang, Y. Xu, H.F. Liu, J. Huang, X. Zhang, H. Liu, J. Cheng, C.J. Tang, Destabilization and nonlinear interaction of tearing modes in tokamak plasmas with locally reversed shear, 27 (2020) 114501.
[33] Z.-X. Wang, L. Wei, X. Wang, Y. Liu, Self-suppression of double tearing modes via Alfvén resonance in rotating tokamak plasmas, Physics of Plasmas, 18 (2011) 050701.
[34] X.Q. Wang, X.G. Wang, W. Xu, Z.X. Wang, Interlocking and nonlinear saturation of double tearing modes in differentially rotating plasmas, Physics of Plasmas, 18 (2011) 012102.
[35] J. Wang, Z.X. Wang, L. Wei, Y. Liu, Control of neo-classical double tearing modes by differential poloidal rotation in reversed magnetic shear tokamak plasmas, Nuclear Fusion, 57 (2017) 046007.
[36] R.B. Zhang, X.Q. Lu, Q.H. Huang, J.Q. Dong, X.Y. Gong, Effect of toroidal plasma rotation on double tearing modes in cylindrical geometry, Physics of Plasmas, 23 (2016) 122509.
[37] T. Liu, Z.X. Wang, J.L. Wang, L. Wei, Suppression of explosive bursts triggered by neo-classical tearing mode in reversed magnetic shear tokamak plasmas via ECCD, Nuclear Fusion, 58 (2018) 076026.
[38] W. Zhang, Z.W. Ma, S. Wang, Hall effect on tearing mode instabilities in tokamak, Physics of Plasmas, 24 (2017) 102510.
[39] G. Sun, C. Dong, L. Duan, Effects of electron cyclotron current drive on the evolution of double

tearing mode, Physics of Plasmas, 22 (2015) 092509.
[40] W. Zhang, Z.W. Ma, X.Q. Lu, H.W. Zhang, Influence of shear flows on dynamic evolutions of double tearing modes, Nuclear Fusion, 60 (2020) 126022.
[41] T. Liu, Z.R. Wang, M.D. Boyer, S. Munaretto, Z.X. Wang, B.H. Park, N.C. Logan, S.M. Yang, J.K. Park, Identification of multiple eigenmode growth rates towards real time detection in DIII-D and KSTAR tokamak plasmas, Nuclear Fusion, 61 (2021) 056009.
[42] W. Tang, Z.-X. Wang, L. Wei, J. Wang, S. Lu, Control of neoclassical tearing mode by synergetic effects of resonant magnetic perturbation and electron cyclotron current drive in reversed magnetic shear tokamak plasmas, Nuclear Fusion, 60 (2020) 026015.
[43] W. Zhang, Z.W. Ma, F. Porcelli, H.W. Zhang, X. Wang, Sawtooth relaxation oscillations, nonlinear helical flows and steady-state m/n=1 magnetic islands in low-viscosity tokamak plasma simulations, Nuclear Fusion, DOI (2020).
[44] H.W. Zhang, J. Zhu, Z.W. Ma, G.Y. Kan, X. Wang, W. Zhang, Acceleration of three-dimensional Tokamak magnetohydrodynamical code with graphics processing unit and OpenACC heterogeneous parallel programming, International Journal of Computational Fluid Dynamics, 33 (2019) 393-406.
[45] M. Wu, Z. Liu, T. Zhang, F. Zhong, G. Li, H. Xiang, K. Geng, K. Ye, J. Huang, F. Wen, Y. Wang, X. Han, S. Zhang, H. Liu, G. Li, G. Zhuang, X. Gao, Experimental study of double tearing mode on EAST tokamak, Plasma Science and Technology, 22 (2019) 025102.
[46] J. DeLucia, S.C. Jardin, A.M.M. Todd, An iterative metric method for solving the inverse tokamak equilibrium problem, Journal of Computational Physics, 37 (1980) 183-204.
[47] C.C. Petty, M.E. Austin, C.T. Holcomb, R.J. Jayakumar, R.J. La Haye, T.C. Luce, M.A. Makowski, P.A. Politzer, M.R. Wade, Magnetic-Flux Pumping in High-Performance, Stationary Plasmas with Tearing Modes, Physical Review Letters, 102 (2009) 045005.
[48] I.T. Chapman, Controlling sawtooth oscillations in tokamak plasmas, Plasma Physics and Controlled Fusion, 53 (2011) 013001.